New Phytologist

Research

Phenolic profile within the fine-root branching orders of an evergreen species highlights a disconnect in root tissue quality predicted by elemental- and molecular-level carbon composition

Jun-Jian Wang[1,2], Nishanth Tharayil[3], Alex T. Chow[1], Vidya Suseela[3] and Hui Zeng[2,4]

[1]The Belle W. Baruch Institute of Coastal Ecology & Forest Science, Clemson University, Georgetown, SC 29442, USA; [2]Shenzhen Key Laboratory of Circular Economy, Shenzhen Graduate School, Peking University, Shenzhen 518055, China; [3]School of Agricultural, Forest and Environmental Sciences, Clemson University, Clemson, SC 29634, USA; [4]College of Urban and Environmental Sciences, Peking University, Beijing 100871, China

Author for correspondence:
Jun-Jian Wang
Tel: +1 843 546 1013
Email: junjiaw@clemson.edu

Received: *5 December 2014*
Accepted: *24 February 2015*

New Phytologist (2015) **206:** 1261–1273
doi: 10.1111/nph.13385

Key words: decomposition, fine roots, lignin, lignin indices, organic matter, phenolics.

Summary

- Fine roots constitute a significant source of plant productivity and litter turnover across terrestrial ecosystems, but less is known about the quantitative and qualitative profile of phenolic compounds within the fine-root architecture, which could regulate the potential contribution of plant roots to the soil organic matter pool.
- To understand the linkage between traditional macro-elemental and morphological traits of roots and their molecular-level carbon chemistry, we analyzed seasonal variations in monomeric yields of the free, bound, and lignin phenols in fine roots (distal five orders) and leaves of *Ardisia quinquegona*.
- Fine roots contained two-fold higher concentrations of bound phenols and three-fold higher concentrations of lignin phenols than leaves. Within fine roots, the concentrations of free and bound phenols decreased with increasing root order, and seasonal variation in the phenolic profile was more evident in lower order than in higher order roots. The morphological and macro-elemental root traits were decoupled from the quantity, composition and tissue association of phenolic compounds, revealing the potential inability of these traditional parameters to capture the molecular identity of phenolic carbon within the fine-root architecture and between fine roots and leaves.
- Our results highlight the molecular-level heterogeneity in phenolic carbon composition within the fine-root architecture, and imply that traits that capture the molecular identity of the root construct might better predict the decomposition dynamics within fine-root orders.

Introduction

Fine roots (≤ 2 mm in diameter) are critical components of plant architecture as they take up nutrients and water which are vital for maintaining plant productivity across ecosystems (Lynch, 1995; Rewald *et al.*, 2011; Freschet *et al.*, 2013; Warren *et al.*, 2015). Fine roots account for *c.* 48% of the net primary productivity in mature forest ecosystems (Freschet *et al.*, 2013), and their production and turnover regulate soil nutrient cycling and atmospheric carbon (C) sequestration (Jackson *et al.*, 1997; Norby & Luo, 2004; Norby *et al.*, 2004; Iversen, 2010). While leaf litter largely decomposes on the soil surface, resulting in only a small proportion of the degradation products entering soils (Prescott, 2010), the turnover and decomposition of roots represent an important pathway for the formation of soil organic matter (SOM) (Bird *et al.*, 2008; Mendez-Millan *et al.*, 2010; Mambelli *et al.*, 2011). However, large 'invisible' uncertainty in root dynamics, including root production, survival, and decomposition, has significantly hindered our ability to accurately forecast the root-derived C and nutrient cycling in terrestrial ecosystems (Matamala *et al.*, 2003; Luo *et al.*, 2004; Hobbie *et al.*, 2010; Iversen *et al.*, 2015).

Although > 65% of C sequestered in soil is derived from fine roots (Richter *et al.*, 1999; Pritchard *et al.*, 2008), we still lack a comprehensive understanding of the complexity in the construction of roots that regulates their decomposition. Traditional elemental ratios (e.g. the carbon-to-nitrogen ratio [C : N]) that predict the decomposition of leaf litter fail to forecast the propensity for decomposition of fine roots (Silver & Miya, 2001; Hobbie *et al.*, 2010; De Graaff *et al.*, 2013), and meta-analysis of global data estimates that the decomposition of fine-root litter proceeds 2.8 times more slowly than the decomposition of leaf litter from the same plant species (Freschet *et al.*, 2013). Similarly, a dichotomy exists within the fine-root orders in terms of morphology and construct. Contrary to the traditional view that considers fine roots as homogenous entities, recent studies show that fine roots have significant heterogeneity within the branching architecture, and the distal roots (or the lower order roots)

commonly have smaller root diameter and length (Pregitzer *et al.*, 1997), higher specific root area and specific root length (Wang *et al.*, 2012), a lower stele proportion (Guo *et al.*, 2008), a higher mycorrhizal colonization rate (Guo *et al.*, 2008), a higher N concentration (Pregitzer *et al.*, 2002), a lower C (also cellulose) concentration (Guo *et al.*, 2004), greater absorption ability (Rewald *et al.*, 2011), a higher respiration rate (Xia *et al.*, 2010), and shorter longevity (Wells *et al.*, 2002). Such heterogeneity in root morphology and physiology is also reflected in the decomposition susceptibility within fine-root orders. Despite a higher N concentration, a lower [C : N], a high specific root area, and nonwoody structure, which collectively should facilitate microbe-mediated mineralization, the lower order roots commonly have a lower rate of decomposition than the woody higher order roots. This unusual pattern of root decomposition has been reported across multiple species and ecosystems in which the branching-order specific decomposition of fine roots has been investigated (Fan & Guo, 2010; Goebel *et al.*, 2011; Olajuyigbe *et al.*, 2012; Sun *et al.*, 2013; Xiong *et al.*, 2013; Wang *et al.*, 2014). This challenges the current paradigm that links elemental ratios to the decomposability of below-ground plant tissues (Hobbie *et al.*, 2010). This disconnect could be attributable to differences in the chemical construct of the root tissues, as highlighted by the compound-specific decomposition of aboveground tissues (Manzoni *et al.*, 2008; Suseela *et al.*, 2013, 2014a).

Despite their lower abundance compared with polysaccharides, phenolic compounds exert a disproportionate influence in conferring recalcitrance to plant tissues. Phenolic compounds can exist as nonassociated forms in cell vacuoles (free phenols), or can be bound to cell wall components through ester/ether linkages (bound phenols), or can form the structural matrix of lignin (lignin phenols). While free phenols contribute to plant defense and nutrient foraging (Hattenschwiler & Vitousek, 2000), phenolic compounds that crosslink lignins to the cellulose matrix increase the overall recalcitrance of the plant tissues (Boerjan *et al.*, 2003). The slower decomposition of lower order roots exhibits a negative correlation with the acid-unhydrolyzable fraction in these roots (Xiong *et al.*, 2013), which is often operationally defined as 'gravimetric lignin' (Preston *et al.*, 2006, 2009). Similarly, within the first and second root orders, pigmented roots decompose more slowly than nonpigmented white roots (Goebel *et al.*, 2011), indicating the potential influence of polyphenolic depositions in regulating root decomposition. These observations suggest that, within fine roots, the more ephemeral lower order roots that decompose more slowly are a crucial contributor to SOM (Fan & Guo, 2010). However, less is known about the possible differences in the chemical profile within the fine-root architecture and its temporal variation, which could be instrumental in accurately forecasting root decomposability.

As they occupy the soil environment, which is laden with pathogens and toxins, roots rely on heteropolymers such as lignins, suberins and tannins to protect tissues from harmful microbes and chemicals (Cooper & Owensmith, 1985; Bernays *et al.*, 1989; Hagerman & Butler, 1991; Hobbie, 2000). Fine roots have a lower abundance of suberin as they are primarily involved in the uptake of water and nutrients, but may have a higher abundance of polyphenolic compounds, including tannins and lignins, which have protective functions and provide the structural rigidity necessary for navigation of the heterogeneous soil matrix. Based on the function of the roots, the heteropolymeric composition of roots is also expected to change across seasons and developmental stages. As the remobilization of the structural matrix is limited, polyphenolic compounds undergo relative enrichment during root senescence and thus could interfere with the further decomposition of the root tissues. For example, the relative abundance of lignin, one of the most slowly decomposing components in plant biomass (Hobbie, 2000; Boerjan *et al.*, 2003; Suseela *et al.*, 2013), could increase the recalcitrance of roots. Thus, investigating the phenolic profile and its seasonal variation in root and leaf could be instrumental in understanding how the molecular identity of C varies between these tissues, and across seasons, which might partly explain the observed disconnect in the decomposability of roots and leaves predicted using traditional elemental parameters.

The molecular identity and arrangement of phenolic compounds within the tissue matrix can be of greater importance than their total quantity in plant defense (Tharayil *et al.*, 2011). The specific functions and turnover rates of root orders could give rise to distinctive phenolic profiles within fine roots, and if such variations are consistent, the phenolic biomarkers could then be used to identify different orders of fine roots. Monomeric phenol biomarkers have been widely used in recent decades in organic geochemistry and ecology. For example, pioneering research has demonstrated that such biomarkers are helpful in tracing the sources and fates of terrestrial and marine dissolved/deposited organic matter (Goni & Hedges, 1995; Hedges *et al.*, 1997; Benner, 2004; Tesi *et al.*, 2012); they have also been used to evaluate the decomposition of plant tissue and the subsequent contribution of plant-derived compounds to SOM (Hedges *et al.*, 1988; Benner *et al.*, 1991; Goni *et al.*, 1993; Opsahl & Benner, 1995; Otto & Simpson, 2006a; Nierop & Filley, 2007; Kuo *et al.*, 2008; Pisani *et al.*, 2013). Several classic phenol indices have been widely adopted as biomarkers, such as the ratio of syringyl : vanillyl phenols (S: V) to differentiate lignin sources of angiosperm and gymnosperm origin (Ertel *et al.*, 1984), the ratio of cinnamyl : vanillyl phenols (C: V) to differentiate woody and nonwoody sources (Hedges *et al.*, 1986), and the ratio of acid to aldehyde of vanillyl (Ad : Al(V)) and syringyl (Ad : Al(S)) phenols to evaluate the diagenetic state of lignin in natural samples (Hedges *et al.*, 1988). Other useful indices such as the 3,5-dihydroxybenzoic acid to vanillyl phenol ratio (Bd: V) (Prahl *et al.*, 1994) for organic matter degradation and the lignin phenol vegetation index (LPVI) for taxonomic source identification of organic matter have also been proposed (Tareq *et al.*, 2004). Similarly, the catalytic efficiency of lignin-degrading peroxidase enzymes has recently been linked to phenol indices of SOM, which indicates the potential of phenol ratios in predicting tissue decomposability (Triebwasser-Freese *et al.*, 2015). To our knowledge, no previous research has explored the use of various phenol indices to identify specific root orders.

Considering the potential abundance, function, and dynamicity of phenolic compounds in roots, we hypothesized that: (1) similar to macro-elemental and morphological traits, the

fine-root architecture will exhibit heterogeneity in the content and association of phenolic compounds within the root matrix; (2) the molecular-level phenolic composition and association across fine-root orders will be independent of their respective macro- elemental and morphological traits; and (3) compared with higher order roots, lower order roots will exhibit higher temporal variation in their phenolic chemistry because of their faster turnover rates. We tested the above hypotheses by analyzing the seasonal dynamics of phenolic compounds in roots and leaves of *Ardisia quinquegona*, a shrub species with the most rapid increase in number in the forest community succession at Dinghu Mountain in South China, the first established subtropical nature reserve in China (Zhou *et al.*, 2004).

Materials and Methods

Study site and sample collection

Dinghu Mountain in South China (23°09′21″–23°11′30″N, 112°30′39″–112°33′41″E; 1155 hectares) has a mean temperature of 28°C in summer and 12.6°C in winter, and mean annual precipitation of 1926 mm. The soil type in the study area is latosolic red soil, with surface SOM ranging from 2.94% to 4.27% (Wang *et al.*, 2012). The coniferous and broad-leaved mixed forest accounts for 46.4% of the area of the nature reserve after more than half a century of succession from the pure *Pinus massoniana* forest planted between the 1930s and 1950s. *Ardisia quinquegona* Blume is a species that has become dominant in the herb layer (where it is the second most abundant species), the shrub layer (fourth most abundant species), and the tree layer (seventh most abundant species) (Zhou *et al.*, 2004). Root samples were collected on six occasions, in January, April, June, August, October and November in 2010, and in January in 2011, from plots (400 m^2) on a 35° south-facing slope (23°09′38.5″N, 112°32′28.9″E), with an elevation of between 200 and 300 m above mean sea level. On each sampling occasion, three to five mature shrubs that were > 3 m high with a diameter at breast height (DBH) > 3 cm were randomly selected. For the root collection, we adopted the intact soil block (30 cm × 20 cm × 10 cm; length × width × depth) method (Guo *et al.*, 2004) to obtain five to 10 complete root systems from each shrub with largest diameter > 5 mm (containing more than five branching orders). All sequential root collection was from another soil block not far away from the previous sampling block (< 1 m distance) next to the same labeled plants to guarantee that the roots were from the same source. For leaf samples, 20–30 well-grown intact leaves were randomly selected from each plant. All samples were placed in labeled bags on ice, and frozen within 12 h of collection.

Sample pretreatment and root trait determination

The frozen roots in the soil block were unfrozen at a low temperature and rinsed with low-temperature deionized water (*c.* 1°C) three to five times to remove the soil. Any remaining soil attached to the roots was examined under a microscope at magnification 10× and removed carefully using forceps. According to the branching-order classification (Fitter, 1982; Pregitzer *et al.*, 2002), the most lateral roots were defined as first-order roots; roots from which two first-order roots branched were classified as second-order roots, and so on. The roots were carefully separated using forceps based on branch order, and the diameter and length of individual roots were measured under a microscope (Motic SMZ-140 Series, Xiamen, China) at magnification 1000× for roots of the first order ($n > 100$), second order ($n > 100$), third order ($n > 50$), fourth order ($n = 10$) and fifth order ($n = 10$). The biomass of individual roots after drying (50°C) was recorded. Tissue density (TD), specific root area (SRA), and specific root length (SRL) of different orders were also calculated.

The leaves were washed with Milli-Q water at low temperature to remove any dust on the leaf surface. All roots and leaves were dried (50°C), ground, sieved (through 200 mesh; 0.074 mm), and kept at −20°C before analysis. The total C and N concentrations of samples were measured using an elemental analyzer (Vario EL Cube; Elementar, Hanau, Germany; Wang *et al.*, 2012).

Sequential extraction of phenolics

The phenolic fractions (free phenols, bound phenols and lignin phenols) have different biological significance; for example, the unbound vacuolar fraction of phenolic compounds is involved in the regulation of the redox state of a cell and in the synthesis of polymeric phenols, whereas the bound phenolic fractions cross-link the lignin matrix to cellulose and thus provide rigidity to the tissue/organs. Hence, while the free-phenolic fraction may exhibit some innate recalcitrance to decomposition at the molecular level, the bound fraction and the lignin matrix increase resistance to decomposition at the tissue/organ level. Thus, separation of various phenolic pools through sequential extraction of plant samples could provide greater insight into tissue carbon quality (Martens, 2002; Suseela *et al.*, 2014b) that regulates the decomposition of plant tissues. We used sequential extraction to separate the phenolic compounds into these three fractions (Fig. 1) following the method of Tamura & Tharayil (2014), with modifications. The ester/ether-bound phenols are recovered following a mild-base hydrolysis that cleaves these cross-linkages. The phenolic compounds that constitute the lignin matrix are seldom perturbed by mild-base hydrolysis and require oxidative degradation at a higher temperature and pressure in the presence of CuO (Hedges & Ertel, 1982).

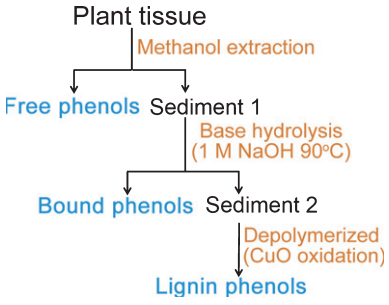

Fig. 1 Schematic of the sequential extraction of phenolic compounds from plant tissue to obtain different operational fractions.

For the free-phenol fraction, 50.0 mg of sample was extracted by shaking for 3 h with 2.5 ml of methanol in 8-ml glass tubes on a rotary shaker at room temperature (20°C). After centrifugation (1500 ***g*** for 15 min), 1.5 ml of supernatant was transferred to amber GC vials and stored at −20°C. The remaining supernatant was discarded, and the pellet was washed with 2.5 ml of methanol twice and then dried at 50°C overnight.

For the bound-phenol fraction, the methanol-extracted pellet was hydrolyzed with 6 ml of freshly prepared 1 M NaOH (pre-sparged with Ar for 30 min) in 8-ml glass tube. Potential oxidation of compounds was further minimized by maintaining an Ar atmosphere in headspace during the hydrolysis. The tubes were incubated in a water bath at 90°C for 3 h in the dark. After cooling in an ice bath, the tubes were centrifuged and 4 ml of the supernatant was transferred to a new glass tube. The residual pellet was washed twice with 5 ml of deionized water, dried and stored for the lignin analysis. To 4 ml of hydrolysate, 50 µl of *trans*-cinnamic acid (CiAD) and ethyl vanillin (EVAL; both 400 mg l^{-1}) was added as internal standards and 2 ml of 50% HCl was added to reduce the pH to < 2. The tubes were then centrifuged and the precipitate was discarded. The solution in the tubes was cooled at 4°C for 20 min and extracted by shaking with 2 ml of ethyl acetate on a rotary shaker for 15 min and cooled for another 20 min at 4°C to facilitate phase separation. The tubes were then centrifuged and 1 ml of the ethyl acetate layer was transferred into GC vials and stored at −20°C.

The lignin fraction was oxidatively depolymerized in 23 ml of Acid Digestion Vessels model 4749 (Parr Instrument Co., Moline, IL, USA), adopting a similar method as in Kaiser & Benner (2012). The base hydrolyzed pellet was combined with 500 mg of CuO, 75 mg $Fe(NH_4)_2(SO4)_2{\cdot}6H_2O$ and 5 ml of freshly prepared 2 M NaOH (pre-sparged with Ar for 30 min) in Teflon cups. The tubes were rinsed with 5 ml of 2 M NaOH twice and transferred to the Teflon cup. The cup was sparged again with Ar for *c.* 3 min and immediately capped. The vessel was carefully sealed and incubated at 155°C for 160 min. At the end of the incubation, the vessels were rapidly cooled in an ice bath to room temperature. The digestion mixture was transferred to 50-ml centrifuge tubes and internal standards were added as above. Approximately 1.5 ml of 24 N H_2SO_4 was added to each tube to adjust the pH to < 2, and the tubes were gently shaken (*c.* 5–10 min). The tubes were centrifuged and 12 ml of supernatant was transferred to a clean glass tube. The depolymerized lignin-derived phenols were recovered using liquid–liquid extraction with 2 ml of ethyl acetate at 4°C, and 1 ml of ethyl acetate layer was stored in a GC vial at −20°C. During the above sequential extractions, the samples and solutions were kept away from direct light, and the temperature was maintained below 4°C, unless specified otherwise. Parallel blanks were also extracted following the same procedures for quality assurance and quality control.

Phenol derivatization and GC-MS quantification

Twelve phenolic monomers including *p*-hydroxybenzoic acid (PAD), *p*-hydroxyacetophenone (PON), *p*-hydroxybenzaldehyde (PAL), vanillic acid (VAD), acetovanillone (VON), vanillin (VAL), ethyl vanillin (EVAL), syringic acid (SAD), acetosyringone (SON), syringaldehyde (SAL), cinnamic acid (CiAD), *p*-coumaric acid (CAD), ferulic acid (FAD) and 3,5-dihydroxybenzoic acid (DiOHBA) were measured in all three phenol fractions. The samples of three fractions were derivatized using *N*-methyl-*N*-methyl-*N*- (trimethylsilyl)- triflouroacetamide with 1% trimethylchlorosilane (MSTFA + 1% TMCS) before analysis using GC-MS. Combination of TMCS with MSTFA facilitates a more efficient and complete silylation of active hydrogen groups in the analyte. For the derivatization, 200 µl of extracted sample was transferred to 300-µl low-volume vials and dried under an N_2 stream. Then 100 µl of derivatization reagent was added, vortexed and incubated at 65°C for 25 min. The derivatized samples were analyzed within 8 h. One or two microliters of each sample was injected using a 10 : 1 split into a gas chromatograph coupled to a single quadrupole mass spectrometer (GC/MS Agilent 7890 system + Agilent 5975C mass detector; Santa Clara, CA, USA). Helium was used as a carrier gas with a constant flow rate of 1.2 ml min^{-1}. The temperature of the injection port was maintained at 270°C and the source and quad temperatures were set at 150 and 240°C, respectively. The separation of phenolic compounds was attained using a DB5-MS column (30 m × 250 µm × 0.25 µm; J&W Scientific, Folson, CA, USA). The initial oven temperature was maintained at 80°C for 2 min, ramped at 10°C min^{-1} to 260°C. Both Scan (range *m/z* 100–400) and SIM mode were used for identification and quantification. The blank and standard recovery tests were conducted for QA/QC. The limit of detection (LoD) for each of the 12 phenols ranged from 0.01 to 0.1 mg l^{-1}, the recovery ranged from 91 to 117%, and the relative standard deviations for blanks and standards were both within ± 5%.

Calculation of indices and statistical analyses

Excluding the internal standards (CiAD and EVAL), the sum of the other 12 phenols was calculated as Σ12 phenolics and the carbon-normalized yield was noted as Λ12. Four classes of phenols were also calculated: *p*-hydroxyl (P = PAD + PON + PAL), vanillyl (V = VAD + VON + VAL), syringyl (S = SAD + SON + SAL), and cinnamyl phenols (C = CAD + FAD). The yield of eight lignin-derived phenols ($V + S + C$) was calculated and noted as Λ8. As V phenols contribute to recalcitrant C-C linkages, the proportion of vanillyl units in Λ8 was calculated as V:Λ8 (Triebwasser-Freese *et al.*, 2015). The lignin phenol vegetation index (LPVI) was calculated as $[S\%(S\%+1)/(V\%+1)+1] \times [C\%(C\%+1)/(V\%+1)+1]$ according to Tareq *et al.* (2004), where V%, S%, and C% are the percentages of V, S, and C in Λ8.

The significance of differences in all macro-elemental (C concentration, N concentration, and [C : N]), morphological (root diameter, root length, specific root area, specific root length, and tissue density), and phenolic traits (P, V, S and C phenol yield, Λ12, Λ8, V:Λ8, S:V, C:V, Ad : Al(V), Ad : Al(S), Bd:V and LPVI) among roots of the first five orders and leaves (except morphological traits for leaves) were determined using ANOVA followed by Dunnett's *t*-test as the samples were paired by sampling

time. Based on the similarity from cluster analysis (Ward's method; squared Euclidean distance; Guo *et al.*, 2013) of all the traits captured in our study, the root orders were categorized into lower order roots (first three orders) and higher order roots (root orders 4 and 5). The significance of differences in all traits among lower order roots, higher order roots, and leaves was determined using ANOVA followed by Tukey's honestly significant difference test. Pearson's correlation coefficients were calculated among root traits for all root samples, as the data were normally distributed. A principal component analysis (PCA) was used to analyze the relationships among the standardized 21 root traits as the Kaiser-Mayer-Olkin measure (overall and individual >0.8) and Bartlett's tests ($P < 0.001$) passed. Four components were extracted, which explained 48.1%, 21.3%, 11.2% and 6.4%, respectively, and 86.9% of the total variance (Supporting Information Table S1). The component scores for all samples were calculated on each of the principal components (Table S2). All statistical analyses were conducted using SPSS 15.0 for Microsoft Windows (SPSS Inc., Chicago, IL, USA) and the level of significance for all analyses was set at 0.05.

Results

Root morphological and macro-elemental traits

In *A. quinquegona*, root diameter and root length consistently increased from the first to the fifth orders, conferring the lower order roots (root orders 1–3; R1–R3) with higher specific root area and specific root length compared with the higher order roots (root orders 4 and 5; R4 and R5; Table 1). Chemically, the C concentration ([C]) generally increased and the N concentration ([N]) consistently decreased with root order, resulting in a consistent increase in the elemental C to N ratio ([C : N]) with root order (first order: 28.6 ± 0.7 mean $\pm$ SE; fifth order: 65.8 ± 3.1). Although root [C], [N], and [C : N] did not vary with season ($P > 0.1$), there was a consistent decrease in root [C : N] from August to October and the lowest root [C] was observed in October for all five branch orders (Fig. 2).

Variation in phenolic profiles among fine-root orders

The yield of free phenols consistently decreased as root order increased at each sampling time (Figs 3a, 4a). Across all root orders, VAD, SAD, and DiOHBA were the most abundant mono-phenolic compounds in the methanol extracts, and phenol abundance always followed: *V* phenols > *S* phenols > *P* phenols > *C* phenols. Within *P*, *V* and *S* phenols, the relative abundance of phenols followed: acid > aldehyde > ketone (Fig. 3a). The variation in the composition of phenolic monomers (*V*: *S*: *P*: *C* or acid : aldehyde : ketone) was greater in lower order roots compared with higher order roots.

The yield of bound phenols generally decreased with increasing root order, except for the first-order roots which had slightly lower VAD and SAD yields than the second-order roots. FAD did not exhibit a definite trend with root order (Fig. 4b). Thus, Λ12 of the bound phenols also decreased with increasing root order (Fig. 4b). FAD was the most abundant among the 12 monomeric phenols (accounting for 22.6–48.8%) in all root samples, followed by the aldehyde or acid of *S* or *V* phenols. The phenolic ketones were less abundant than the respective aldehydes or acids in all *P*, *V* and *S* phenols (Fig. 3b).

For the lignin fraction, the yields of *P* and *C* phenols and DiOHBA appeared to decrease with root order (Fig. 3c). However, we did not observe such a consistent decreasing trend with root order for *V* and *S* phenols, which were the major components of the 12 phenols (accounting for 93.9–97.7%). Within the distal three orders, most of the monomeric phenols and Λ12 showed decreasing trends with increasing root order.

Seasonal variation in root phenolics

The Λ12 of all phenol fractions across all root orders was highly season-dependent ($P < 0.05$), except for free phenols ($P = 0.22$). For the free and bound fractions, the root samples in October presented rather different patterns compared with other months. The Λ12 of the free-phenol fraction (all < 400 μg g-C^{-1} except for the first order in October) showed an increasing trend from August to October for roots of the distal three orders ($P < 0.05$; Fig. 4a), but appeared to be relatively stable for the higher order roots (i.e. the fourth- and fifth-order roots; $P = 0.67$) across seasons. For the bound fraction, the Λ12 ranged from 2.57 to 5.09 mg g-C^{-1} and had distinct troughs in October for both all orders and the distal three orders ($P < 0.01$; Fig. 4b). For the lignin fraction, the Λ12 ranged from 16.3 to 41.8 mg g-C^{-1} among the different root orders across different times of collection (Fig. 4c). Roots collected in October had a significantly lower lignin-phenol yield than roots collected in January, April, and June ($P < 0.01$; Fig. 4c). Roots of the distal three orders had a higher lignin-phenol yield in June than in August and October ($P < 0.01$; Fig. 4c).

Difference between roots and leaves

Across seasons, leaves showed distinct chemical dynamics compared with roots, and there was no correlation in the seasonal patterns between leaves and roots for [C], [N], [C : N], and Λ12 of free phenols, bound phenols, lignin phenols and total phenols (all $P > 0.05$). Quantitatively, the leaves had both higher [C] and [N] than all fine roots, and comparable [C : N] (27.5 ± 1.3) to the first-order roots. The root samples consistently had a higher yield of structural phenols than leaves (Fig. 4), including both the bound (*c.* 2 times) and lignin phenols (*c.* 3 times).

Phenol indices

The lower order roots (R1–R3), higher order roots (R4–R5), and leaf samples differed in the composition of monomeric phenols. The *S*: *V* of total phenols followed: R1–R3 (3.07 ± 0.23) > R4–R5 (2.14 ± 0.13) > leaves (1.45 ± 0.04), whereas the *C*: *V* followed: leaves (0.65 ± 0.09) > R1–R3 (0.30 ± 0.03) > R4–R5 (0.21 ± 0.01) (Fig 5a). For different phenol fractions, the lower order roots, higher order roots, and leaves were located in

Table 1 The morphological and chemical properties of the roots of different orders and leaf samples

Trait	Abbreviation	Indicator for	Units	R1	R2	R3	R4	R5	Leaf
Elemental carbon concentration	[C]	C abundance	%	44.3 ± 0.4e	44.3 ± 0.4e	45.1 ± 0.3d	46.0 ± 0.2c	47.2 ± 0.3b	48.2 ± 0.2a
Elemental nitrogen concentration	[N]	N abundance	%	1.82 ± 0.04b	1.71 ± 0.06c	1.43 ± 0.08d	1.01 ± 0.07e	0.85 ± 0.04f	2.10 ± 0.10a
Elemental carbon : nitrogen ratio	[C : N]	Nutritive value of tissues	–	28.6 ± 0.7e	30.5 ± 1.0d	37.5 ± 2.2c	55.0 ± 4.2b	65.8 ± 3.1a	27.5 ± 1.3e
Root diameter	Diameter	Common morphological traits reflecting root functions	mm	0.42 ± 0.05e	0.53 ± 0.08d	0.74 ± 0.09c	1.08 ± 0.08b	1.59 ± 0.14a	–
Root length	Length		cm	1.02 ± 0.43e	2.39 ± 1.00d	5.51 ± 1.73c	15.2 ± 3.8b	22.3 ± 5.2a	–
Specific root area	SRA		$cm^2\ g^{-1}$	265 ± 20ab	311 ± 22a	250 ± 12b	123 ± 3c	81.7 ± 7.7d	–
Specific root length	SRL		$m\ g^{-1}$	20.1 ± 0.9a	18.2 ± 0.8b	10.7 ± 0.1c	3.64 ± 0.05d	1.63 ± 0.03e	–
Tissue density	TD	Density of root construct	$g\ cm^{-3}$	0.36 ± 0.02a	0.24 ± 0.01c	0.22 ± 0.02d	0.30 ± 0.02b	0.31 ± 0.03b	–
Total 12 phenol yield	Λ12	Abundance of total monophenols	mg g-C^{-1}	33.3 ± 2.9a	31.9 ± 3.3a	26.6 ± 1.8b	28.2 ± 2.4ab	28.6 ± 1.5ab	8.77 ± 0.50c
Total lignin phenol yield	Λ8	Abundance of monophenols that constitute lignin	mg g-C^{-1}	31.3 ± 2.9a	30.2 ± 3.3ab	25.4 ± 1.9b	27.1 ± 2.4ab	27.8 ± 1.5ab	7.65 ± 0.52d
p-hydroxy phenol yield	*P*	Abundance of *P* phenols	mg g-C^{-1}	1.16 ± 0.08a	0.96 ± 0.04b	0.72 ± 0.04c	0.67 ± 0.06c	0.50 ± 0.03d	0.59 ± 0.02d
Vanillyl phenol yield	*V*	Abundance of *V* phenols	mg g-C^{-1}	6.93 ± 0.63b	7.31 ± 0.88ab	5.76 ± 0.43c	8.28 ± 0.64a	8.13 ± 0.48ab	2.45 ± 0.21d
Syringyl phenol yield	*S*	Abundance of *S* phenols	mg g-C^{-1}	22.4 ± 2.26a	21.0 ± 2.4ab	17.8 ± 1.7b	17.1 ± 1.6b	18.0 ± 1.1b	3.69 ± 0.36c
Cinnamyl phenol yield	*C*	Abundance of *C* phenols	mg g-C^{-1}	2.00 ± 0.13a	1.92 ± 0.13ab	1.75 ± 0.12b	1.75 ± 0.14b	1.64 ± 0.15bc	1.50 ± 0.09c
Vanillyl : lignin phenol ratio	*V* : Λ8	Lignin quality	–	0.20 ± 0.01c	0.23 ± 0.01c	0.22 ± 0.02c	0.31 ± 0.01b	0.28 ± 0.02b	0.36 ± 0.01a
Syringyl : vanillyl phenol ratio	*S* : *V*	Index for angiosperm or gymnosperm source	–	3.18 ± 0.10a	2.87 ± 0.14a	3.15 ± 0.38a	2.04 ± 0.09b	2.23 ± 0.16b	1.45 ± 0.04c
Cinnamyl : vanillyl phenol ratio	*C* : *V*	Index for woody or nonwoody source	–	0.30 ± 0.04b	0.28 ± 0.03b	0.31 ± 0.03b	0.21 ± 0.01c	0.20 ± 0.01c	0.65 ± 0.09a
Acid : aldehyde for vanillyl phenols	Ad : Al(*V*)	Diagenetic state of lignin	–	0.18 ± 0.02a	0.18 ± 0.03a	0.21 ± 0.02a	0.12 ± 0.01b	0.13 ± 0.01b	0.13 ± 0.02b
Acid : aldehyde for syringyl phenols	Ad : Al(*S*)	Diagenetic state of lignin	–	0.09 ± 0.01a	0.11 ± 0.03a	0.10 ± 0.01a	0.08 ± 0.01ab	0.08 ± 0.00b	0.09 ± 0.01a
3,5-dihydroxybenzoic acid : vanillyl phenols	*Bd* : *V*	Degradation status	%	7.15 ± 0.49b	6.7 ± 0.82b	7.33 ± 0.69b	4.23 ± 0.41c	3.47 ± 0.16c	9.12 ± 1.47a
Lignin phenol vegetation index	LPVI	Taxonomic source identification	–	739 ± 117b	615 ± 85b	777 ± 162b	329 ± 32c	353 ± 44c	1090 ± 239a

Values are mean ± SE. Different letters after means indicate a significant difference ($P < 0.05$). R1–R5 refer to fine-root categories from first order to fifth order.

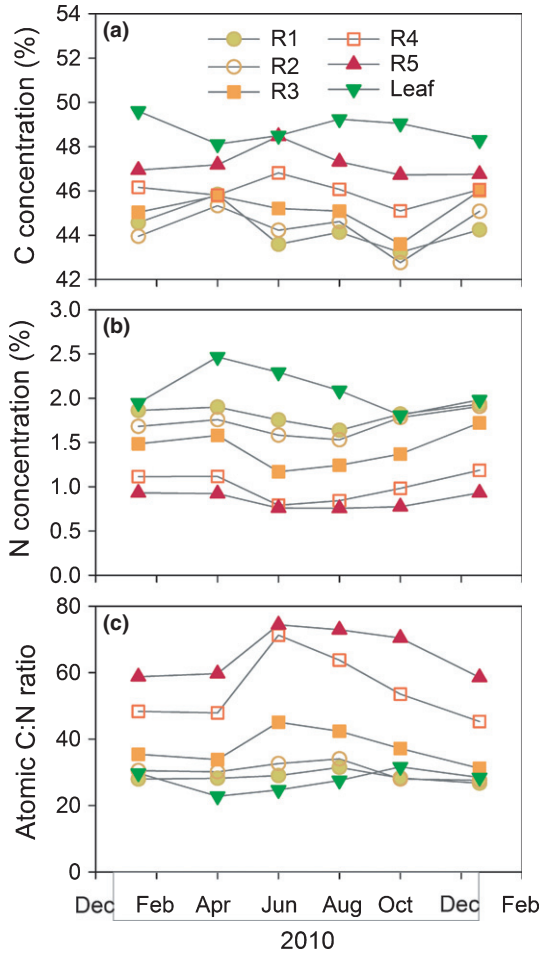

Fig. 2 Seasonal variation in (a) carbon (C), (b) nitrogen (N), and (c) carbon:nitrogen ratio (C : N) in roots and leaves of *Ardisia quinquegona*. Each data point represents the mean of three replicates. R1–R5 refer to fine-root categories from first order to fifth order.

different regions in the S: V vs C: V plot (Fig. 5b). For free phenols, leaf samples had higher C: V (1.13 ± 0.56) and lower S: V (0.31 ± 0.07) than roots (overall S: V: 0.84 ± 0.08; C: V: 0.25 ± 0.03). Bound phenols had a relatively narrow S: V range but a wide C: V range for all samples (Fig. 5b), with an S: V ranking of leaves (0.61 ± 0.02) < R4–R5 (0.72 ± 0.03) < R1–R3 (0.82 ± 0.03), and a C: V ranking of R1–R3 (1.23 ± 0.07) < R4–R5 (1.59 ± 0.14) < leaves (4.73 ± 0.41). Lignin phenols had a wide S: V range but a relatively narrow C: V range, with an S: V ranking of leaves (1.62 ± 0.05) < R4–R5 (2.32 ± 0.15) < R1–R3 (3.63 ± 0.09), and a C: V ranking of higher order roots (0.041 ± 0.004) < R1–R3 (0.091 ± 0.013) < leaves (0.14 ± 0.02).

Across seasons, Ad : Al was highest in August for both leaves and the distal three orders of roots (Fig. 5c). Ad : Al(V) of total phenols was higher in R1–R3 than R4–R5 and leaves ($P < 0.01$) (Fig. 5c, Table 1). Different phenol fractions had rather different Ad : Al, with a ranking of free phenols (*c.* 1–8) > bound phenols (*c.* 0.5–3) > lignin phenols for all samples ($P < 0.001$; Fig. 5d). There were significant differences in the Ad : Al of free phenols and the Ad : Al(V) of bound phenols between higher and lower order roots, but not for lignin phenols. The V: $A8$ followed R1–R3 < R4–R5 < leaves. For both Bd: V and LPVI, R1–R3 had higher values compared with R4–R5 (Table 1). Compared with roots, leaves exhibited a higher Bd: V value but lower LPVI (Table 1).

Multivariate analysis

The common root morphological and macro-elemental traits did not correlate with most of the root phenol yields (all correlation coefficients < 0.4, except for *P* phenol yield; Table S3). The morphological and macro-elemental traits were independent of root phenol yields as they exhibited differential loadings on the two principal component axes (Fig. 6a; Table S1). Further, R1–R3 and R4–R5 clustered differently across PC axis 1, which explained 48.1% of the variation. The root orders R4–R5 had higher elemental C, C : N, root length and diameter and relative proportion of vanillyl units, whereas R1–R3 had higher elemental N, specific root length and area, and all other phenol ratios including LPVI (Fig. 6b).

Discussion

In this study, we unambiguously demonstrated seasonal and molecular-level heterogeneity in phenolic composition between the roots and leaves and within the fine-root branching architecture of an evergreen shrub. Despite a similar [C : N] between lower order roots and leaves, the three times higher lignin-phenol yield and two times higher bound-phenol yield in fine-root orders than leaves could explain the slower decomposition of roots of this species (J-J. Wang *et al.*, unpublished data). The pattern of higher yields of free and bound phenols in the distal fine-root orders observed in this study, if also found across other species, could partly explain the field-observed slower decomposition of lower order roots of several tree species despite their higher N content compared with higher-order roots (Fan & Guo, 2010; Goebel *et al.*, 2011; Olajuyigbe *et al.*, 2012; Sun *et al.*, 2013; Xiong *et al.*, 2013; Wang *et al.*, 2014). Given the critical roles of phenolic compounds in tissue construct, SOM formation, and C and N biogeochemistry, our results provide insightful implications for the role of phenolics in the functioning and decomposition of fine roots.

Heterogeneity in the composition of phenolics in roots: implications for root functions

The fine roots of *A. quinquegona* exhibited significant branching-order-dependent patterns in the concentration, composition, and indices of phenols, that is, decreasing trends for free phenols and bound phenols with increasing root order. These results are clearly suggestive of molecular heterogeneity of phenolic C within fine-root systems, which is in agreement with our first hypothesis. The three fractions of phenols have different roles in the root construct and rhizosphere functions. The free-phenolic compounds are important component of root exudates and help plants in the active acquisition of mineral nutrients, especially metal ions, through chelation, pH reduction and redox

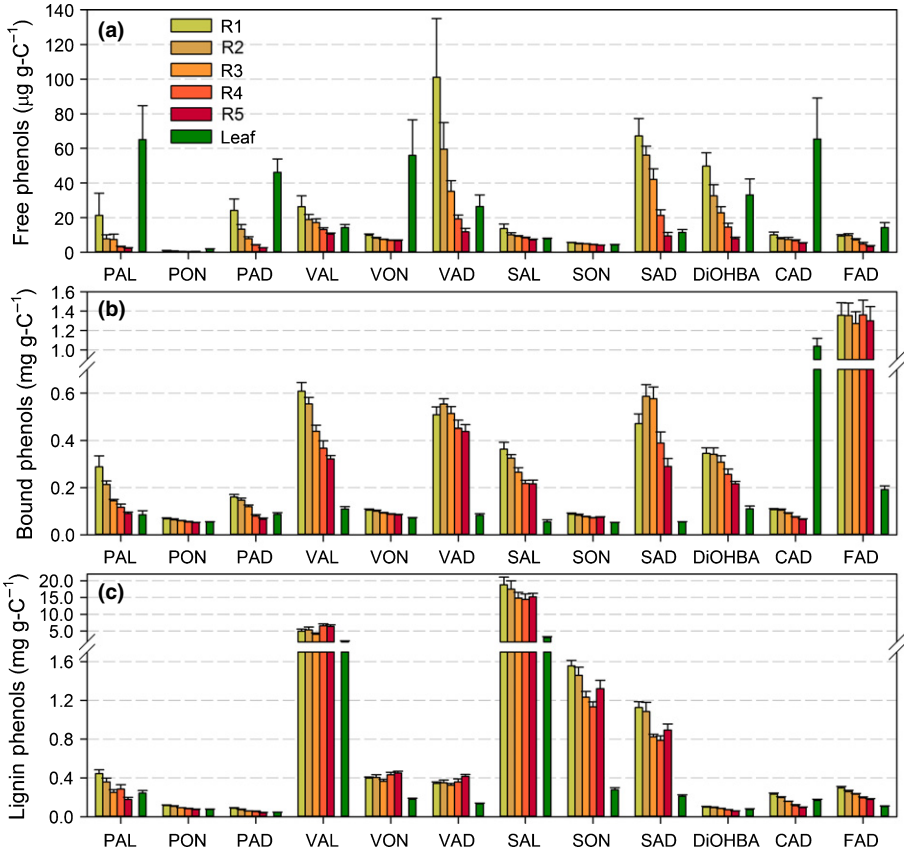

Fig. 3 The carbon-normalized amount of 12 monomeric phenols in the (a) free, (b) bound, and (c) lignin fractions of root and leaf samples. Bars represent mean ± SE ($n = 6$). The 12 phenolic monomers are: PAL, *p*-hydroxybenzaldehyde; PON, *p*-hydroxyacetophenone; PAD, *p*-hydroxybenzoic acid; VAL, vanillin; VON, acetovanillone; VAD, vanillic acid; SAL, syringaldehyde; SON, acetosyringone; SAD, syringic acid; DiOHBA, 3,5-dihydroxybenzoic acid; CAD, *p*-coumaric acid; FAD, ferulic acid. R1–R5 refer to fine-root categories from first order to fifth order.

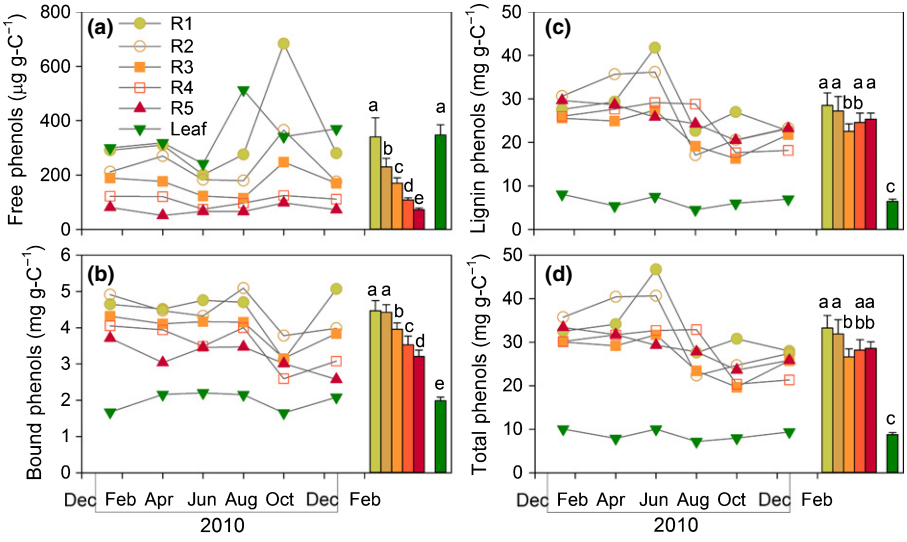

Fig. 4 Seasonal variation in the sum of the yield of 12 phenols (Λ12) in (a) free phenols, (b) bound phenols, (c) lignin phenols, and (d) total phenols of root and leaf samples. The bar graph represents mean ± SE across six sampling periods (left to right: R1–R5 and leaf). Letters at the top of each bar indicate significantly different groups. R1–R5 refer to fine-root categories from first order to fifth order.

alterations (Tharayil, 2009; McNear, 2013). Thus, the decreasing free-phenol yield with increasing root order may reflect the lesser involvement of higher order fine roots in exudate-mediated active nutrient foraging (Wang *et al.*, 2012; Guo *et al.*, 2013). As a consequence of their ability to deter pest/pathogen attack, free phenols could also act as defense compounds in young roots during the formative stage before significant lignification occurs (Beckman, 2000). The phenolic cross-linkages within lignocellulose and the limited suberin matrix would contribute to the bound phenols measured in this study (Lam *et al.*, 2001). The bound phenols are important in the early stages of litter decomposition as they cross-link lignins with the cell wall and thus serve as a structural barrier that impedes microbial access to labile C compounds (e.g. polysaccharides and proteins; Austin & Ballare, 2010; Suseela *et al.*, 2014a). Also, cross-linking hydrophobic phenols with the hydrophilic polysaccharide components of cell walls greatly enhance the hydrophobicity of vascular tissue to guarantee high hydraulic conductivity and water uptake efficiency (Sarkanen & Ludwig, 1971; Baxter *et al.*, 2009), especially for the lower order roots (Rewald *et al.*, 2011). In contrast to the distribution

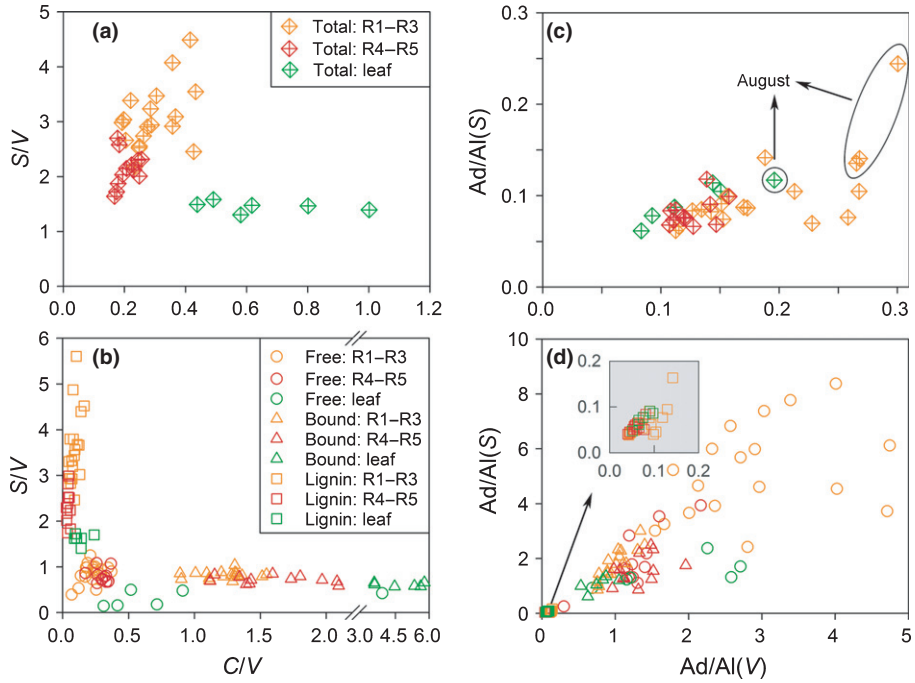

Fig. 5 The phenol index diagrams for (a, c) total and (b, d) fractional phenols in root and leaf samples. Relationship between *C* : *V* (cinnamyl : vanillyl phenols) and *S* : *V* (syringyl : vanillyl phenols) are represented in (a) and (b). Total yields of phenol monomer units: vanillyl (vanillin + acetovanillone + vanillic acid); syringyl (syringaldehyde + acetosyringone + syringic acid); cinnamyl (*p*-coumaric acid + ferulic acid) units. (b) and (c) represent acid to aldehyde ratios for vanillyl Ad : Al(*V*) and syringyl phenols Ad : Al(*S*). R1–R5 refer to fine-root categories from first order to fifth order.

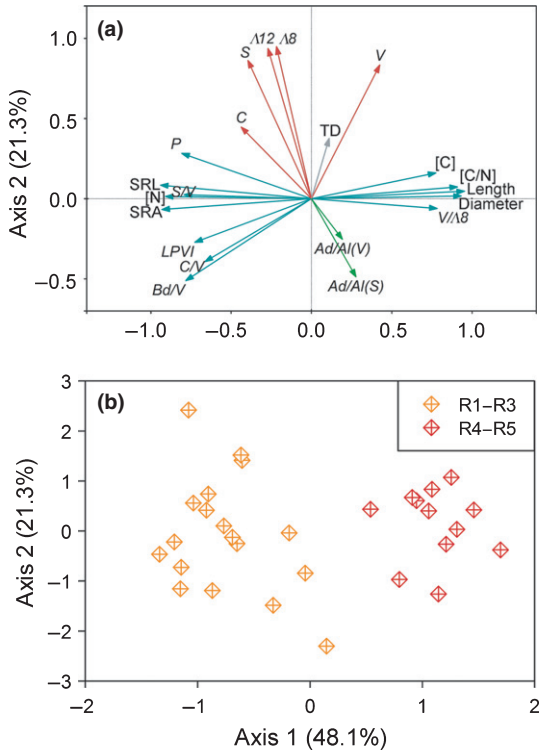

Fig. 6 Principal component analysis (PCA) for root morphological, macro-chemical, and phenolic traits of fine-root samples. (a) Trait loadings show the first two principal components, and the blue, red, green, and gray arrows show high loading in the first four sequential principal components, respectively. (b) The component scores of the lower order and higher order roots on the first two principal components. R1–R5 refer to fine-root categories from first order to fifth order. See Table 1 for an explanation of abbreviations.

patterns of the free and bound phenols, the C-normalized concentration of lignin phenols, which provide the structural framework of the roots, were similar across the root orders (Fig. 4). The similar abundance of lignin phenols across root orders might partly reflect the rigidity of the root construct required to overcome the mechanical resistance of the soil matrix to root navigation. Despite this similar content of lignins, the lower order roots may be more resistant to microbial degradation as a result of better integration of lignin within the root matrix, as evident from their higher content of phenolic cross-linkers (bound phenols).

Both correlation analyses (Table S3) and PCA (Fig. 6a) suggested that the measured phenol yields (*V*, *S*, *C*, *Λ*8 or *Λ*12, except *P*) were probably independent of root morphological or macro-chemical traits, which is in agreement with our second hypothesis. This result suggests that the root morphological or macro-elemental traits could not directly capture the molecular-level C composition within the fine-root architecture. The *P* phenols correlated significantly with the root morphological or macro-chemical traits, possibly because *p*-hydroxybenzaldehyde and *p*-hydroxybenzoic acid could be derived from sources other than lignin, such as tannins (Otto & Simpson, 2006b). The higher relative abundance of *S* phenols (advanced end-products with higher construction costs per molecule; Boerjan *et al.*, 2003) than *V* phenols in lower order roots (Fig. 5a) reflects a potential change in the biosynthesis of lignin monomers along root orders. As the C5 of the aromatic ring is not available for a coupling reaction in *S* phenols, this higher abundance of *S* phenols than *V* phenols in lower order roots could contribute to more β-O-4 inter-unit linkages (Boerjan *et al.*, 2003). These aryl-ether linkages are less rigid compared with C-C inter-unit linkages in *V*-phenol-abundant lignins, thus providing greater structural flexibility in lower order roots.

Seasonal variation in phenol composition in fine-root orders

We observed active root growth in April and greater root senescence in October, which was consistent with the previous observation that there was lower live root biomass and higher root

necromass in October at this study site (Wen *et al.*, 1999). The relatively low leaf N concentration (as an index of photosynthetic activity; Evans, 1989) in October (Fig. 2) indicated a potentially low supply of photosynthates for root growth later in the season. The decreasing root [C : N] from August to October (Fig. 2) also suggest that some of the C fraction in roots was being resorbed. Yet, in contrast to leaf aging/senescence, the root samples did not show an obvious decrease in [N] (Fig. 2), suggesting that the plants retrieved less N from fine roots during senescence. We propose that the observed lack of extensive N resorption from roots could partly be attributable to the fact that a larger portion of N in roots is contributed by transmembrane carrier- and channel-proteins that are actively involved in the uptake and intercellular transport of resources (Tischner, 2001). Inaccessibility of proteins, which are embedded in the membrane (intrinsic proteins), to proteases could hinder their resorption during senescence (Thomas *et al.*, 2002). In contrast, Rubisco, the most abundant protein in leaves, is a soluble extrinsic membrane protein and hence is more vulnerable to breakdown resorption during leaf senescence. Additionally, the warmer and subtropical climate with less seasonal variation in temperatures may also have contributed to the observed lower dynamics of N concentration in fine roots. Trees in northern temperate climates experiencing distinct seasons have shown decrease in root N concentration later in the growing season (Xia *et al.*, 2010; Jia *et al.*, 2011; Zadworny *et al.*, 2015).

Notably, the yield of bound phenols decreased from August to October during root senescence, while the yield of free phenols in lower order roots sharply increased (Fig. 4). It is highly likely that, during the resorption that precedes the senescence of roots, the bound phenolic compounds are actively cleaved by plant esterases (Melillo *et al.*, 1992) resulting in the observed increase in free phenols. As the bound phenols are mostly cross-linked to the structural polysaccharides through ester and glycosidic linkages (Iiyama *et al.*, 1994), the breakdown of labile polysaccharides during the early stage of root senescence (Fukuda, 1996) may also lead to the remobilization of bound phenols. This theory is supported by the observation that the lower order roots, which have a shorter life-span (Wells *et al.*, 2002; Xia *et al.*, 2010; McCormack & Guo, 2014), exhibited the highest spike in free phenols from August to October (Fig. 4a), and is in agreement with our third hypothesis that lower order roots would exhibit higher temporal variation in their phenolic profile.

By contrast, the root lignin phenols did not show a consistent change across the seasons for different root orders (Fig. 4c), probably as a result of the strong ether and C-C linkages within the lignin phenols which are relatively resistant to enzymatic cleavage. Across different root orders, the higher order roots maintained a much less fluctuating phenol profile compared with the lower order roots (Fig. 4), indicating a much slower turnover rate and relatively stable biochemistry for higher order roots.

Variation in phenol indices with root order and season

During lignin degradation, side-chain oxidation of monomeric phenols can increase Ad : Al for both vanillyl and syringyl species (Hedges *et al.*, 1988; Opsahl & Benner, 1995; Otto & Simpson, 2006a). Extensive investigations have revealed that Ad : Al(V) and Ad : Al(S) are reliable indicators of the diagenetic degree of organic matter. For example, Hedges *et al.* (1988) reported that the Ad : Al increased from 0.14 in undegraded tissues to as high as 0.51 for wood degradation. Opsahl & Benner (1995) found that Ad : Al increased by *c.* 1.2–2.8 times (from *c.* 0.2–0.4 to *c.* 0.4–0.9) after 4 yr of decomposition for green bald cypress (*Taxodium distichum*) needles and mangrove (*Avicennia germinuns*) leaves. The Ad : Al values of the distal three root orders were season-dependent and were highest in August, which could have been caused by high temperatures in summer oxidizing more phenols to acids (Paul, 2006; Feng *et al.*, 2008). Although all the samples were from live biomass, Ad : Al showed large variation across root orders (0.09–0.21 on average; Table 1), suggesting that such indices should be used with caution to indicate the diagenetic degree of subsamples from root branches (even all < 2 mm) or from soils that contain large amounts of fine roots.

Ecological implications of the molecular identity of carbon in roots and leaves

Both leaves and fine roots are important biomass with fast turnover rates that form the precursors of SOM (O'Brien & Iversen, 2009). Although the leaves and the first-order roots of the studied species had similar elemental [C : N] values, they differed significantly in their phenolic composition. The roots had two to four times higher structural phenol yield compared to leaves (Fig. 4), implying that the lower order roots of the studied species have a much higher potential than leaves to resist microbial degradation and contribute to SOM (Bird *et al.*, 2008; Mambelli *et al.*, 2011; Tamura & Tharayil, 2014). It should be noted that, within leaves, the petioles and veins often exhibit differential molecular chemistry from the rest of the lamina. Thus, the decomposition pattern of leaves could also show high tissue-dependent variability (Filley *et al.*, 2008; Crow *et al.*, 2009). Future studies on the molecular-level C quality of different plant tissues across several plant species would extend our knowledge of plant physiological functions and biogeochemical cycling.

Within the fine-root orders, recent studies have widely reported that ephemeral fine roots (nonwoody lower order roots), despite their lower [C : N] and higher specific root area (greater accessibility to microorganisms in soil), decomposed much more slowly than longer lived roots (Fan & Guo, 2010; Goebel *et al.*, 2011). The C quality reflected by various phenol fractions could be more important than [C : N] in controlling the decomposition of fine roots. For example, despite similar lignin contents, compared to higher-order roots, we observed a higher abundance of ester-bound phenolics in lower-order roots, which may enhance the integrity of the nonphenolic root-tissue matrix through cross-linkages with lignin. Extensive phenol cross-linkages, along with the transmembrane nature of proteins in roots, could make the N in these tissues less accessible to microbes, thus hindering the decomposition of lower order roots despite their lower [C : N]. Commonly, across plant species, lower order roots are often lower in cellulose content (Dornbush *et al.*, 2002; Guo

et al., 2004). If this is the case for *A. quinquegona*, the observed trend in bound phenols and lignin content will result in a higher phenol-to-cellulose ratio in lower order roots of this study species, which would in turn facilitate extensive integration of cellulose with the lignin matrix, and thus a greater recalcitrance of distal fine roots. For example, compared with pure cellulose, a small fraction (*c.* 5%) of the lignin in the cellulose matrix could significantly enhance the recalcitrance of biomass to enzymatic degradation, and decrease the decomposition rate by half (Austin & Ballare, 2010). Within the fine-root architecture, as the root lifespan is known to increase geometrically with increasing branch order, and as the root lignin phenol concentration in lower order roots is either comparable to or higher than that in higher order roots, we can conclude that the flux of phenols to the SOM pool would be higher from lower order than from higher order roots for *A. quinquegona*.

Molecular-level carbon quality of fine roots: implications for modeling

Although fine roots represent one of the most dynamic plant organs with regard to their response to the environment, they remain the most simplistic component of many terrestrial biosphere models (Iversen, 2010; Smithwick *et al.*, 2014; Iversen *et al.*, 2015). In terrestrial biosphere models, many ecosystem processes are simplified to simulate these processes at broad spatial and temporal scales (Warren *et al.*, 2015). However, for models to be accurate in their predictions, such simplifications should be built on a mechanistic understanding of those processes at much finer scales (Schulze, 2014). The large-scale models that simulate biogeochemical cycling (e.g. CLM 4.5 BGC) in Earth System Models parameterize root decomposition and allocate root litter to different soil pools based on the C and N contents of roots (Iversen *et al.*, 2015). The heterogeneity of phenolic composition within the fine-root orders captured in our study, combined with the results from recent field-level fine-root decomposition experiments, suggests that the molecular-level identity of the root C might exert an overriding influence in shaping the recalcitrance within different fine-root orders. Thus, irrespective of the [C : N], the higher abundance of free and bound phenols in lower order roots could be more critical in predicting root decomposability. To further simplify the branching-order-based classification, recent studies have proposed that fine roots be categorized into an ephemeral absorptive pool and a longer lived transport fine-root pool based on their distinct morphology, life span, mycorrhizal colonization, and respiration (Xia *et al.*, 2010; McCormack *et al.*, 2015). The variation in phenolic profile within fine-root orders captured in our study strongly supports this proposed classification. Our analyses show that finer roots can be further grouped into lower order (R1–R3) and higher order (R4–R5) with respect to the ratio abundance of phenolics and various phenolic indices (Table 1; Figs 5a, 6b). This bifurcation, which effectively captures the chemical profiles within fine-root orders, would provide higher resolution to the current single-root pools in biogeochemical models without adding to model complexity. Overall, our results suggest that the molecular-level composition of C has the potential to provide valuable insights into fine-root dynamics in terrestrial ecosystems and could be used to better parameterize root decomposition in large-scale models.

Acknowledgements

We thank the three anonymous reviewers and Drs Richard Norby and Luke McCormack for their valuable and thoughtful comments. We also thank Mr Sen-Lu Yin for help with sampling and assistance in elemental analyses. This study received financial support from the Natural Science Foundation of China through an award to H.Z. (31321061) and the Department of Energy (DOE) Office of Science award (DE-SC0010832) to N.T. V.S. gratefully acknowledges the National Science Foundation Postdoctoral Research Fellowship in Biology (DBI-1306607). This project was also based on work supported by USDA-NIFA (project number SC-1700489). Technical contribution number 6344 of the Clemson University Experimental Station. J-J.W. appreciates financial support from the China Scholarship Council (CSC [2011]3010).

References

Austin AT, Ballare CL. 2010. Dual role of lignin in plant litter decomposition in terrestrial ecosystems. *Proceedings of the National Academy of Science, USA* **107**: 4618–4622.

Baxter I, Hosmani PS, Rus A, Lahner B, Borevitz JO, Muthukumar B, Mickelbart MV, Schreiber L, Franke RB, Salt DE. 2009. Root suberin forms an extracellular barrier that affects water relations and mineral nutrition in Arabidopsis. *Plos Genetics* **5**: e1000492.

Beckman CH. 2000. Phenolic-storing cells: keys to programmed cell death and periderm formation in wilt disease resistance and in general defence responses in plants? *Physiological and Molecular Plant Pathology* **57**: 101–110.

Benner R. 2004. What happens to terrestrial organic matter in the ocean? *Marine Chemistry* **92**: 307–310.

Benner R, Fogel ML, Sprague EK. 1991. Diagenesis of belowground biomass of *Spartina-Alterniflora* in salt-marsh sediments. *Limnology and Oceanography* **36**: 1358–1374.

Bernays EA, Cooper-Driver GA, Bilgener M. 1989. *Herbivores and plant tannins.* San Diego, CA, USA: Academic Press.

Bird JA, Kleber M, Torn MS. 2008. ^{13}C and ^{15}N stabilization dynamics in soil organic matter fractions during needle and fine root decomposition. *Organic Geochemistry* **39**: 465–477.

Boerjan W, Ralph J, Baucher M. 2003. Lignin biosynthesis. *Annual Review of Plant Biology* **54**: 519–546.

Cooper SM, Owensmith N. 1985. Condensed tannins deter feeding by browsing ruminants in a South-African savanna. *Oecologia* **67**: 142–146.

Crow SE, Filley TR, McCormick M, Szlavecz K, Stott DE, Gamblin D, Conyers G. 2009. Earthworms, stand age, and species composition interact to influence particulate organic matter chemistry during forest succession. *Biogeochemistry* **92**: 61–82.

De Graaff M-A, Six J, Jastrow JD, Schadt CW, Wullschleger SD. 2013. Variation in root architecture among switchgrass cultivars impacts root decomposition rates. *Soil Biology and Biochemistry* **58**: 198–206.

Dornbush ME, Isenhart TM, Raich JW. 2002. Quantifying fine-root decomposition: an alternative to buried litterbags. *Ecology* **83**: 2985–2990.

Ertel JR, Hedges JI, Perdue EM. 1984. Lignin signature of aquatic humic substances. *Science* **223**: 485–487.

Evans JR. 1989. Photosynthesis and nitrogen relationships in leaves of C_3 plants. *Oecologia* **78**: 9–19.

Fan PP, Guo DL. 2010. Slow decomposition of lower order roots: a key mechanism of root carbon and nutrient retention in the soil. *Oecologia* **163**: 509–515.

Feng XJ, Simpson AJ, Wilson KP, Williams DD, Simpson MJ. 2008. Increased cuticular carbon sequestration and lignin oxidation in response to soil warming. *Nature Geoscience* **1**: 836–839.

Filley TR, McCormick MK, Crow SE, Szlavecz K, Whigham DF, Johnston CT, van den Heuvel RN. 2008. Comparison of the chemical alteration trajectory of *Liriodendron tulipifera* L. leaf litter among forests with different earthworm abundance. *Journal of Geophysical Research. Biogeosciences* **113**: g01027.

Fitter AH. 1982. Morphometric analysis of root systems: application of the technique and influence of soil fertility on root system development in two herbaceous species. *Plant, Cell & Environment* **5**: 313–322.

Freschet GT, Cornwell WK, Wardle DA, Elumeeva TG, Liu WD, Jackson BG, Onipchenko VG, Soudzilovskaia NA, Tao JP, Cornelissen JHC. 2013. Linking litter decomposition of above- and below-ground organs to plant–soil feedbacks worldwide. *Journal of Ecology* **101**: 943–952.

Fukuda H. 1996. Xylogenesis: initiation, progression, and cell death. *Annual Review of Plant Physiology and Plant Molecular Biology* **47**: 299–325.

Goebel M, Hobbie SE, Bulaj B, Zadworny M, Archibald DD, Oleksyn J, Reich PB, Eissenstat DM. 2011. Decomposition of the finest root branching orders: linking belowground dynamics to fine-root function and structure. *Ecological Monographs* **81**: 89–102.

Goni MA, Hedges JI. 1995. Sources and reactivities of marine-derived organic-matter in coastal sediments as determined by alkaline CuO oxidation. *Geochimica Et Cosmochimica Acta* **59**: 2965–2981.

Goni MA, Nelson B, Blanchette RA, Hedges JI. 1993. Fungal degradation of wood lignins – geochemical perspectives from CuO-derived phenolic dimers and monomers. *Geochimica Et Cosmochimica Acta* **57**: 3985–4002.

Guo DL, Mitchell RJ, Hendricks JJ. 2004. Fine root branch orders respond differentially to carbon source-sink manipulations in a longleaf pine forest. *Oecologia* **140**: 450–457.

Guo DL, Xia MX, Wei X, Chang WJ, Liu Y, Wang ZQ. 2008. Anatomical traits associated with absorption and mycorrhizal colonization are linked to root branch order in twenty-three Chinese temperate tree species. *New Phytologist* **180**: 673–683.

Guo YY, Wang JJ, Kong DL, Wang W, Guo DL, Wang YB, Xie QL, Liu YS, Zeng H. 2013. Fine root branch orders contribute differentially to uptake, allocation, and return of potentially toxic metals. *Environmental Science & Technology* **47**: 11465–11472.

Hagerman A, Butler LG. 1991. Tannins and lignins. In: Rosenthal GA, Berenbaum MR, eds. *Herbivores: their interactions with secondary plant metabolites*. San Diego, CA, USA: Academic Press, 355–388.

Hattenschwiler S, Vitousek PM. 2000. The role of polyphenols in terrestrial ecosystem nutrient cycling. *Trends in Ecology & Evolution* **15**: 238–243.

Hedges JI, Blanchette RA, Weliky K, Devol AH. 1988. Effects of fungal degradation on the CuO oxidation-products of lignin – a controlled laboratory study. *Geochimica Et Cosmochimica Acta* **52**: 2717–2726.

Hedges JI, Clark WA, Quay PD, Richey JE, Devol AH, Santos UD. 1986. Compositions and fluxes of particulate organic material in the Amazon River. *Limnology and Oceanography* **31**: 717–738.

Hedges JI, Ertel JR. 1982. Characterization of lignin by gas capillary chromatography of cupric oxide oxidation-products. *Analytical Chemistry* **54**: 174–178.

Hedges JI, Keil RG, Benner R. 1997. What happens to terrestrial organic matter in the ocean? *Organic Geochemistry* **27**: 195–212.

Hobbie SE. 2000. Interactions between litter lignin and soil nitrogen availability during leaf litter decomposition in a Hawaiian Montane forest. *Ecosystems* **3**: 484–494.

Hobbie SE, Oleksyn J, Eissenstat DM, Reich PB. 2010. Fine root decomposition rates do not mirror those of leaf litter among temperate tree species. *Oecologia* **162**: 505–513.

Iiyama K, Lam TBT, Stone BA. 1994. Covalent cross-links in the cell-wall. *Plant Physiology* **104**: 315–320.

Iversen CM. 2010. Digging deeper: fine-root responses to rising atmospheric CO_2 concentration in forested ecosystems. *New Phytologist* **186**: 346–357.

Iversen CM, Sloan VL, Sullivan PF, Euskirchen ES, McGuire AD, Norby RJ, Walker AP, Warren JM, Wullschleger SD. 2015. The unseen iceberg: plant roots in arctic tundra. *New Phytologist* **205**: 34–58.

Jackson RB, Mooney HA, Schulze ED. 1997. A global budget for fine root biomass, surface area, and nutrient contents. *Proceedings of the National Academy of Sciences, USA* **94**: 7362–7366.

Jia S, Wang Z, Li X, Zhang X, McLaughlin NB. 2011. Effect of nitrogen fertilizer, root branch order and temperature on respiration and tissue N concentration of fine roots in *Larix gmelinii* and *Fraxinus mandshurica*. *Tree Physiology* **31**: 718–726.

Kaiser K, Benner R. 2012. Characterization of lignin by gas chromatography and mass spectrometry using a simplified CuO oxidation method. *Analytical Chemistry* **84**: 459–464.

Kuo LJ, Louchouarn P, Herbert BE. 2008. Fate of CuO-derived lignin oxidation products during plant combustion: application to the evaluation of char input to soil organic matter. *Organic Geochemistry* **39**: 1522–1536.

Lam TBT, Kadoya K, Iiyama K. 2001. Bonding of hydroxycinnamic acids to lignin: ferulic and p-coumaric acids are predominantly linked at the benzyl position of lignin, not the beta-position, in grass cell walls. *Phytochemistry* **57**: 987–992.

Luo YQ, White L, Hui DF. 2004. Comment on "Impacts of fine root turnover on forest NPP and soil C sequestration potential". *Science* **304**: 945c.

Lynch J. 1995. Root architecture and plant productivity. *Plant Physiology* **109**: 7–13.

Mambelli S, Bird JA, Gleixner G, Dawson TE, Torn MS. 2011. Relative contribution of foliar and fine root pine litter to the molecular composition of soil organic matter after in situ degradation. *Organic Geochemistry* **42**: 1099–1108.

Manzoni S, Jackson RB, Trofymow JA, Porporato A. 2008. The global stoichiometry of litter nitrogen mineralization. *Science* **321**: 684–686.

Martens DA. 2002. Identification of phenolic acid composition of alkali-extracted plants and soils. *Soil Science Society of America Journal* **66**: 1240–1248.

Matamala R, Gonzalez-Meler MA, Jastrow JD, Norby RJ, Schlesinger WH. 2003. Impacts of fine root turnover on forest NPP and soil C sequestration potential. *Science* **302**: 1385–1387.

McCormack ML, Dickie IA, Eissenstat DM, Fahey TJ, Fernandez CW, Guo D, Helmisaari H-S, Hobbie EA, Iversen CM, Jackson RB *et al.* 2015. Redefining fine roots improves understanding of belowground contributions to terrestrial biosphere processes. *New Phytologist*. doi: 10.1111/nph.13363

McCormack ML, Guo DL. 2014. Impacts of environmental factors on fine root lifespan. *Frontiers in Plant Science* **5**: a205.

McNear D Jr. 2013. The rhizosphere–roots, soil and everything in between. *Nature Education Knowledge* **4**: 1.

Melillo M, Bleve-Zacheo T, Zacheo G. 1992. Role of peroxidase and esterase isoenzymes in pea roots infected with *Heterodera goettingiana*. *Nematologia Mediterranea* **20**: 171–179.

Mendez-Millan M, Dignac MF, Rumpel C, Rasse DP, Derenne S. 2010. Molecular dynamics of shoot vs. root biomarkers in an agricultural soil estimated by natural abundance ^{13}C labelling. *Soil Biology & Biochemistry* **42**: 169–177.

Nierop KGJ, Filley TR. 2007. Assessment of lignin and (poly-)phenol transformations in oak (*Quercus robur*) dominated soils by ^{13}C-TMAH thermochemolysis. *Organic Geochemistry* **38**: 551–565.

Norby RJ, Ledford J, Reilly CD, Miller NE, O'Neill EG. 2004. Fine-root production dominates response of a deciduous forest to atmospheric CO_2 enrichment. *Proceedings of the National Academy of Sciences, USA* **101**: 9689–9693.

Norby RJ, Luo YQ. 2004. Evaluating ecosystem responses to rising atmospheric CO_2 and global warming in a multi-factor world. *New Phytologist* **162**: 281–293.

O'Brien SL, Iversen CM. 2009. Missing links in the root-soil organic matter continuum. *New Phytologist* **184**: 513–516.

Olajuyigbe S, Tobin B, Hawkins M, Nieuwenhuis M. 2012. The measurement of woody root decomposition using two methodologies in a Sitka spruce forest ecosystem. *Plant and Soil* **360**: 77–91.

Opsahl S, Benner R. 1995. Early diagenesis of vascular plant-tissues – lignin and cutin decomposition and biogeochemical implications. *Geochimica Et Cosmochimica Acta* **59**: 4889–4904.

Otto A, Simpson MJ. 2006a. Evaluation of CuO oxidation parameters for determining the source and stage of lignin degradation in soil. *Biogeochemistry* **80**: 121–142.

Otto A, Simpson MJ. 2006b. Sources and composition of hydrolysable aliphatic lipids and phenols in soils from western Canada. *Organic Geochemistry* **37**: 385–407.

Paul EA. 2006. *Soil microbiology, ecology and biochemistry*. Burlington, MA, USA: Academic Press.

Pisani O, Hills KM, Courtier-Murias D, Simpson AJ, Mellor NJ, Paul EA, Morris SJ, Simpson MJ. 2013. Molecular level analysis of long term vegetative shifts and relationships to soil organic matter composition. *Organic Geochemistry* **62**: 7–16.

Prahl FG, Ertel JR, Goni MA, Sparrow MA, Eversmeyer B. 1994. Terrestrial organic-carbon contributions to sediments on the Washington margin. *Geochimica Et Cosmochimica Acta* **58**: 3035–3048.

Pregitzer KS, DeForest JL, Burton AJ, Allen MF, Ruess RW, Hendrick RL. 2002. Fine root architecture of nine North American trees. *Ecological Monographs* **72**: 293–309.

Pregitzer KS, Kubiske ME, Yu CK, Hendrick RL. 1997. Relationships among roof branch order, carbon, and nitrogen in four temperate species. *Oecologia* **111**: 302–308.

Prescott CE. 2010. Litter decomposition: what controls it and how can we alter it to sequester more carbon in forest soils? *Biogeochemistry* **101**: 133–149.

Preston CM, Nault JR, Trofymow JA. 2009. Chemical changes during 6 years of decomposition of 11 litters in some Canadian forest sites. Part 2. ^{13}C abundance, solid-state ^{13}C NMR spectroscopy and the meaning of "lignin". *Ecosystems* **12**: 1078–1102.

Preston CM, Trofymow JA, Flanagan LB. 2006. Decomposition, $\delta^{13}C$, and the "lignin paradox". *Canadian Journal of Soil Science* **86**: 235–245.

Pritchard SG, Strand AE, McCormack ML, Davis MA, Finzi AC, Jackson RB, Matamala R, Rogers HH, Oren R. 2008. Fine root dynamics in a loblolly pine forest are influenced by free-air-CO_2-enrichment: a six-year-minirhizotron study. *Global Change Biology* **14**: 588–602.

Rewald B, Ephrath JE, Rachmilevitch S. 2011. A root is a root is a root? Water uptake rates of Citrus root orders. *Plant, Cell & Environment* **34**: 33–42.

Richter DD, Markewitz D, Trumbore SE, Wells CG. 1999. Rapid accumulation and turnover of soil carbon in a re-establishing forest. *Nature* **400**: 56–58.

Sarkanen KV, Ludwig CH. 1971. *Lignins: occurrence, formation, structure and reactions*. NewYork, NY, USA: Wiley Interscience.

Schulze ED. 2014. Large-scale biogeochemical research with particular reference to forest ecosystems, an overview. *Forest Ecology and Management* **316**: 3–8.

Silver WL, Miya RK. 2001. Global patterns in root decomposition: comparisons of climate and litter quality effects. *Oecologia* **129**: 407–419.

Smithwick EAH, Lucash MS, McCormack ML, Sivandran G. 2014. Improving the representation of roots in terrestrial models. *Ecological Modelling* **291**: 193–204.

Sun T, Mao ZJ, Han YY. 2013. Slow decomposition of very fine roots and some factors controlling the process: a 4-year experiment in four temperate tree species. *Plant and Soil* **372**: 445–458.

Suseela V, Tharayil N, Xing BS, Dukes JS. 2013. Labile compounds in plant litter reduce the sensitivity of decomposition to warming and altered precipitation. *New Phytologist* **200**: 122–133.

Suseela V, Tharayil N, Xing BS, Dukes JS. 2014a. Warming alters potential enzyme activity but precipitation regulates chemical transformations in grass litter exposed to simulated climatic changes. *Soil Biology & Biochemistry* **75**: 102–112.

Suseela V, Triebwasser D, Linsched N, Morgan J, Tharayil N. 2014b. Effects of warming and elevated CO_2 on the metabolic profiles in leaf litter of photosynthetically divergent grass species. *Ecosphere* **5**: 106.

Tamura M, Tharayil N. 2014. Plant litter chemistry and microbial priming regulate the accrual, composition and stability of soil carbon in invaded ecosystems. *New Phytologist* **203**: 110–124.

Tareq SM, Tanaka N, Ohta K. 2004. Biomarker signature in tropical wetland: lignin phenol vegetation index (LPVI) and its implications for reconstructing the paleoenvironment. *Science of the Total Environment* **324**: 91–103.

Tesi T, Langone L, Goni MA, Wheatcroft RA, Miserocchi S, Bertotti L. 2012. Early diagenesis of recently deposited organic matter: a 9-yr time-series study of a flood deposit. *Geochimica Et Cosmochimica Acta* **83**: 19–36.

Tharayil N. 2009. To survive or to slay: resource-foraging role of metabolites implicated in allelopathy. *Plant Signaling & Behavior* **4**: 580–583.

Tharayil N, Suseela V, Triebwasser DJ, Preston CM, Gerard PD, Dukes JS. 2011. Changes in the structural composition and reactivity of *Acer rubrum* leaf litter tannins exposed to warming and altered precipitation: climatic stress-induced tannins are more reactive. *New Phytologist* **191**: 132–145.

Thomas H, Ougham H, Canter P, Donnison I. 2002. What stay-green mutants tell us about nitrogen remobilization in leaf senescence. *Journal of Experimental Botany* **53**: 801–808.

Tischner R. 2001. Nitrate uptake and reduction in higher and lower plants. *Plant Cell, & Environment* **23**: 1005–1024.

Triebwasser-Freese DJ, Tharayil N, Preston CM, Gerard PG. 2015. Kinetics and activation energy of soil peroxidases across ecosystems of differing lignin chemistries. *Biogeochemistry*. doi:10.1007/s10533-015-0086-3

Wang JJ, Guo YY, Guo DL, Yin SL, Kong DL, Liu YS, Zeng H. 2012. Fine root mercury heterogeneity: metabolism of lower-order roots as an effective route for mercury removal. *Environmental Science & Technology* **46**: 769–777.

Wang W, Zhang XY, Tao N, Ao D, Zeng WJ, Qian YQ, Zeng H. 2014. Effects of litter types, microsite and root diameters on litter decomposition in *Pinus sylvestris* plantations of northern China. *Plant and Soil* **374**: 677–688.

Warren JM, Hanson PJ, Iversen CM, Kumar J, Walker AP, Wullschleger SD. 2015. Root structural and functional dynamics in terrestrial biosphere models – evaluation and recommendations. *New Phytologist* **205**: 59–78.

Wells CE, Glenn DM, Eissenstat DM. 2002. Changes in the risk of fine-root mortality with age: a case study in peach, *Prunus persica* (Rosaceae). *American Journal of Botany* **89**: 79–87.

Wen DZ, Wei P, Kong GH, Ye WH. 1999. Production and turnover rate of fine roots in two lower subtropical forest sites at Dinghushan. *Acta Phytoecologica Sinica* **23**: 74–82.

Xia MX, Guo DL, Pregitzer KS. 2010. Ephemeral root modules in *Fraxinus mandshurica*. *New Phytologist* **188**: 1065–1074.

Xiong YM, Fan PP, Fu SL, Zeng H, Guo DL. 2013. Slow decomposition and limited nitrogen release by lower order roots in eight Chinese temperate and subtropical trees. *Plant and Soil* **363**: 19–31.

Zadworny M, McCormack ML, Wiczyńska K, Jagodzinski AM. 2015. Seasonal variation in root chemistry, but not root morphology, in roots of *Quercus robur* growing in different soil types. *Tree Physiology*. In press

Zhou XY, Huang ZL, Shi JH, Ouyang XJ, Li J, Zhang C. 2004. Short-term dynamics of community composition and structure during succession of coniferous and broad-leaved mixed forest in Dinghushan. *Journal of Tropical and Subtropical Botany* **12**: 323–330.

Supporting Information

Additional supporting information may be found in the online version of this article.

Table S1 Loading of root macro-elemental, morphological, and phenolic traits on the principal components

Table S2 Component scores of root samples based on the principal component analysis

Table S3 The correlation coefficients of the root morphological and chemical properties

Please note: Wiley Blackwell are not responsible for the content or functionality of any supporting information supplied by the authors. Any queries (other than missing material) should be directed to the *New Phytologist* Central Office.